Anisotropy of the Wear Behavior for Carbon Nanotube-Reinforced 6061Al Composites

X. N. Li[1,2] · J. F. Zhang[2] · W. H. Xue[2] · K. Ma[2] · P. Y. Li[2] · Z. Y. Liu[2] · B. L. Xiao[2] · D. R. Ni[2] · Q. Z. Wang[2] · D. Wang[2] · Z. Y. Ma[2]

Abstract

Carbon nanotube (CNT)-reinforced 6061Al (CNT/6061Al) composites with directionally aligned CNT were fabricated, and their wear behavior was investigated. The results indicate that the wear properties of CNT/6061Al composites exhibited a significant anisotropy. A certain CNT concentrations (1 wt% and 2 wt%) could effectively improve the wear resistance of CNT/6061Al composites along the CNT circumferential and CNT radial directions for the load transfer, grain refinement and self-lubrication effect of CNT. The Brass {011} < 211 > and {112} < 110 > textures inhibited the load transfer effect of CNT along the CNT radial direction, resulting in a better wear resistance along CNT circumferential direction than CNT radial direction. Along the CNT axial direction, the weak deformability of composites caused by the intensifying < 111 > fiber texture was the main reasons for the poor wear resistance of CNT/6061Al composites with increasing CNT concentration.

Keywords Carbon nanotube · Metal matrix composite · Wear · Anisotropy

1 Introduction

Carbon nanotubes (CNTs) have been considered as one of the best attractive reinforcements for aluminum matrix composites due to their unique structure and extraordinary properties [1–3]. Experiments and simulations indicated that CNT has extraordinary mechanical properties, for example, the elastic modulus of 1 TPa and strength of 30–100 GPa [4–6], as well as excellent self-lubrication and thermal-electrical conductivity [2]. In recent decades, the research of CNT-reinforced Al (CNT/Al) composites have focused on the mechanical property. Actually, the extraordinary electrical and thermal properties of CNT make the CNT/Al composites potential materials for the application of electric contact current-carrying parts (e.g., armature in the electric contact field) [7, 8]. Obviously, the wear behavior of CNT/Al composites should be focused, besides the conductivity property.

However, most of previous studies demonstrated that CNT/Al composites only exhibited obvious improvement of the wear resistance under a much low loading level [9–14], which was far from the expected level or practical application. This was usually attributed to the weak bearing ability resulting from CNT agglomeration [11, 13], and thus the composites could not take full advantage of the exceptional properties of CNT. This could be proved by our previous finding that the uniformly dispersed CNTs rather than the agglomerated CNTs were beneficial to improve the wear behavior of CNT/6061Al composites [15, 16].

As well known, CNT was quasi 1-D material, which could lead to anisotropy of CNT/Al composites. For example, previous study showed that the best tensile properties of CNT/Al composites were achieved along the direction of aligned CNT due to the strengthening of load transfer [17]. The directionally aligned CNT might also affect the wear behavior of CNT-reinforced composites along different directions. This was verified by previous finding that the directionally aligned CNT/polymer composites showed quite different wear performance along different directions [18]. It should be mentioned that the process for obtaining directionally aligned CNTs in CNT/Al would result in anisotropy of

✉ Z. Y. Liu
zyliu@imr.ac.cn

✉ B. L. Xiao
blxiao@imr.ac.cn

1 School of Materials Science and Engineering, University of Science and Technology of China, Shenyang 110016, China

2 Shi-Changxu Innovation Center for Advanced Materials, Institute of Metal Research, Chinese Academy of Sciences, Shenyang 110016, China

matrix alloy, and the hardness of CNT/Al was much higher than the polymer composites. This means the wear behavior of the CNT/Al composites could be quite different from that of the CNT/polymer composite. Therefore, it is necessary to declare the anisotropic wear resistance of CNT/Al composites, which could provide a basis for future application in electric contact field.

In this study, CNT/6061Al composites with aligned CNTs were prepared through high-energy ball milling (HEM) technology combined with powder metallurgy technology. The effect of CNT orientations (CNT axial, circumferential and radial directions) and concentrations on the wear behavior of CNT/6061Al composites were investigated and analyzed in detail. The aim of present work was to declare the wear anisotropy of CNT/Al composites and reveal the wear mechanisms.

2 Experimental

2.1 Raw Materials and Composites Fabrication

As-received CNTs (purity ~ 98 wt%) with an average outer diameter of 10–20 nm and a length of ~ 5 μm were synthesized using chemical vapor deposition (Fig. 1a). Various mass fractions of CNT were, respectively, milled with 6061Al (Al-1.2 wt% Mg-0.6 wt% Si-0.2 wt% Cu) powders in an attritor (Fig. 1b), conducting at a rotational speed of 400 r/min for 6 h and the ball to powder ratio of 15:1. The milled CNT/6061Al powders were cold-compacted in a cylinder die, degassed and hot pressed at 853 K for 1 h. Then, the hot-pressed billets were hot extruded at 723 K with an

extrusion ratio of 16:1. Finally, the CNT/6061Al composites were solid-solution-treated at 803 K for 2 h, quenched into water at room temperature and then artificial aging treated at 443 K for 6 h (i.e., T6 treatment). For comparison, 6061Al alloy was also fabricated under the same condition.

2.2 Sampling Method and Wear Tests of CNT/6061Al Composites

The sampling method for the wear testing is shown in Fig. 2a. The samples were sectioned along the axis of the extruded rod, the CNTs aligned along the extrusion direction in the extrusion rod and the wear tests were carried out on two different wear surfaces (the red rectangle). During the wear tests, Al_2O_3 ceramic balls slide along different friction directions of CNT axial, CNT circumferential and CNT radial directions, which were marked in Fig. 2b.

The experimental approach of the wear testing is shown in Fig. 3. Wear tests for CNT/6061Al composites were performed using a ball-on-disk type reciprocating sliding wear tester (RTEC MFT-5000) at room temperature. Al_2O_3 ceramic balls with diameter of 4 mm were applied as the wear counterpart. The surface of CNT/6061Al composite disks was polished with 1000 mesh SiC paper, degreased with acetone and dried before testing. The dry sliding tests were performed with a duration of 30 min under a constant condition with a sliding frequency of 10 Hz, an amplitude of 10 mm and an applied load of 10 N. The friction coefficient was given by a computer and the wear rate was calculated by the product of average cross-sectional area of the wear scar, the perimeter of the sliding traces and sliding frequency. The cross-sectional area of the scratches was measured using an
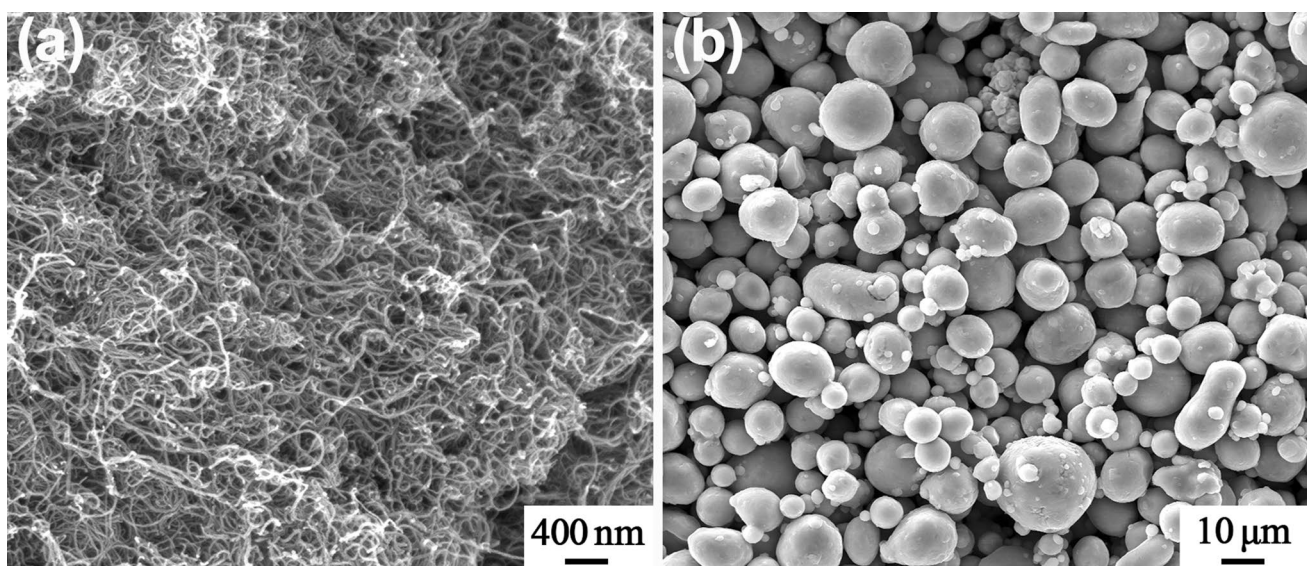

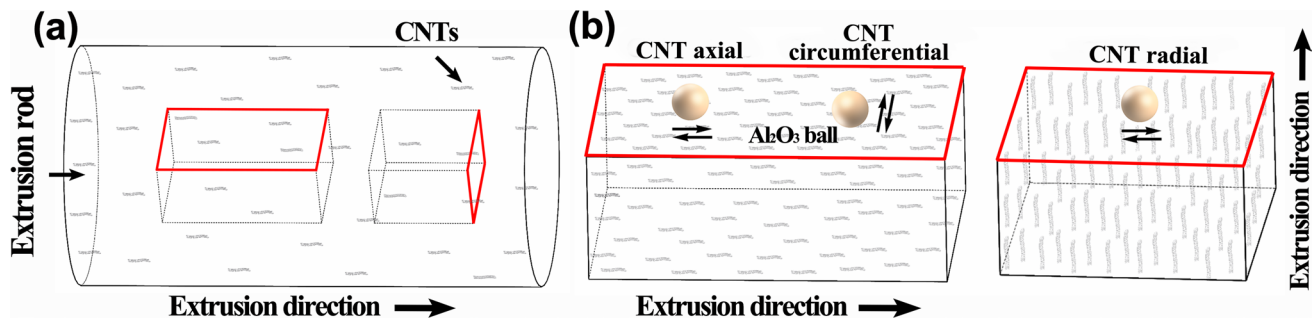**Fig. 1** SEM images of the as-received powders: **a** CNT and **b** 6061Al

Fig. 2 Schematic illustration for **a** sampling method and **b** friction directions of CNT/6061Al composites
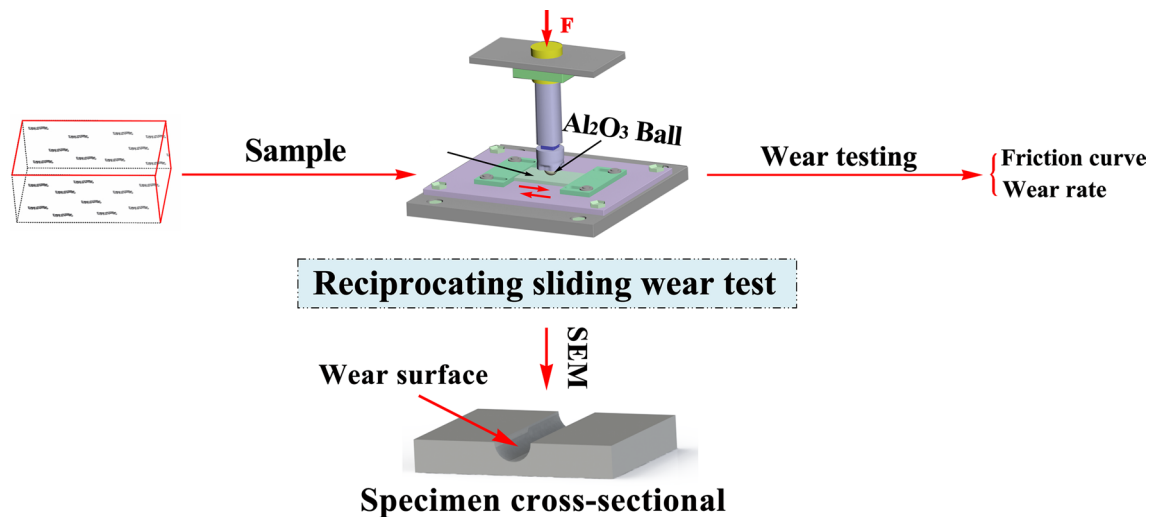

Fig. 3 Schematic of the experimental approach of wear test

Alpha-Step IQ surface profilometer. 15 different areas of scratches were randomly selected to calculate the average cross-sectional area.

2.3 Characterization of Microstructure and Wear

Transmission electron microscope (wt%; Tecnai G2 20) was used to examine the CNT distribution and structure near to the CNT-Al interface. The hardness was measured using a Vickers hardness tester (FM-700, a load of 200 g and a dwell time of 15 s), and eight hardness values were used to obtain an average value for each material. The crystallographic texture was measured using an X-ray diffractometer (XRD, Bruker D8) operated at 3 kW. The specimens used for texture analysis were sectioned along the extruded rod axis and radial directions.

Scanning electron microscopy (SEM, Quanta 450) with energy-dispersive spectroscopy (EDS) facility was used to characterize the wear surface, cross section of wear samples. The 3D morphologies of the wear surfaces were examined by a surface mapping microscope (3D Micro XAM, KLA, USA). The CNT structure damage on the wear surface was characterized by a micro-Raman spectroscopy unit (Jobin Yvon HR800) using a laser wavelength of 532 nm and laser power of 3.2 mW.

2.4 Finite Element Model (FEM) Calculation

The stress distribution of the CNT/Al composites under shear load was studied using FEM calculation. A representative volume element (RVE) of a 2 wt% CNT/6061Al composite was employed to represent the microstructure. The detailed iteration method of the RVE model and the materials properties of each phase could be found in our previous study [19]. Three different shear load conditions were applied on the surfaces of the RVE, to show the influence of the friction direction on the stress distribution. The shear stresses of loads were all set to ~ 50 MPa.

3 Results

3.1 CNT Distribution and Vickers Hardness of CNT/6061Al

Figure 4 shows the images of typical microstructure for the 3 wt% CNT/6061Al composite. It can be seen that the CNTs were uniformly dispersed without obvious clustering (Fig. 4a). Further, the CNTs approximated aligned along the extrusion direction in the 6061Al matrix. That is, the uniformly dispersed CNT/6061Al composites with directionally aligned CNT were prepared successfully. High-resolution image indicates that the interface between CNT and Al matrix was well bonded, and the structure integrity of CNT maintained well (Fig. 4b).

The vickers hardness change of CNT/6061Al composites with different CNT concentrations is shown in Fig. 5a. It can be seen that the hardness increased significantly with the incorporation of CNT, which mainly attributed to the strengthening induced by the uniformly dispersed CNT [20, 21]. Furthermore, the hardness for the surface along the vertical extrusion direction was higher than that along the extrusion direction. Figure 5b shows the ultimate tensile strength (UTS) and elongation to fracture (El) of CNT/6061Al composites with different CNT concentrations. It indicates that the UTS linearly increased, while the El quickly decreased with increasing CNT concentration. These results demonstrate that the strength and hardness of CNT/6061Al composites increased at the cost of the significantly reduced ductility.
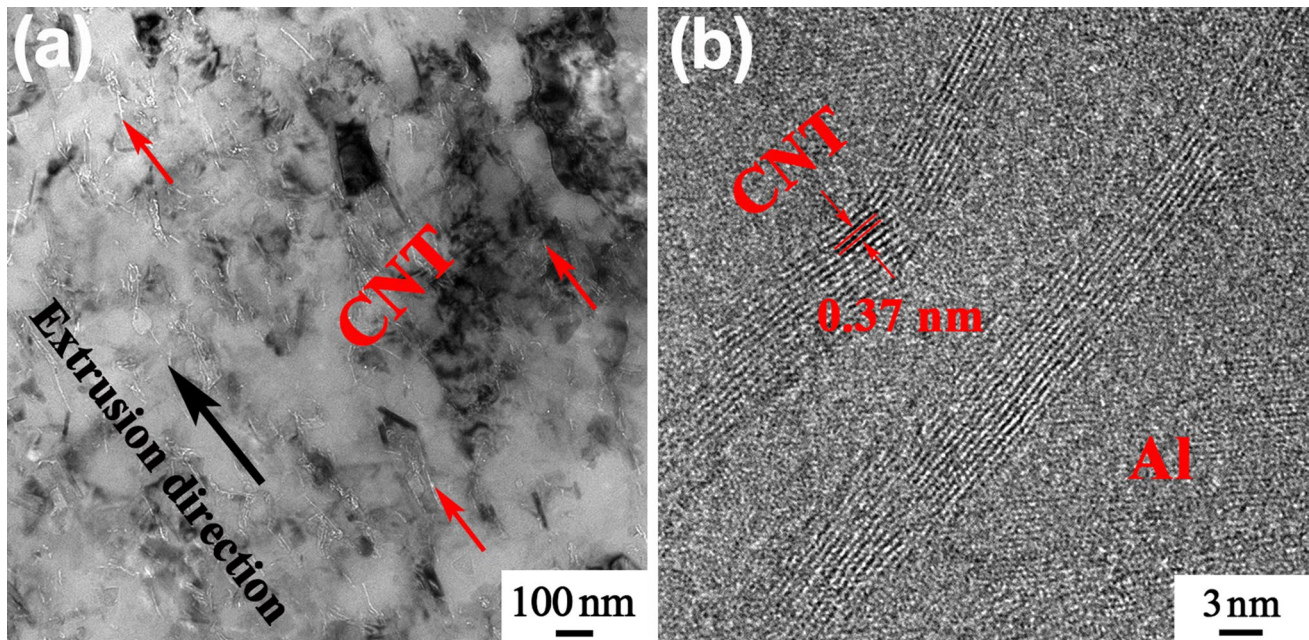

Fig. 4 TEM images: **a** singly dispersed and aligned CNTs; **b** CNT-Al interface in the 3 wt% CNT/6061Al composite
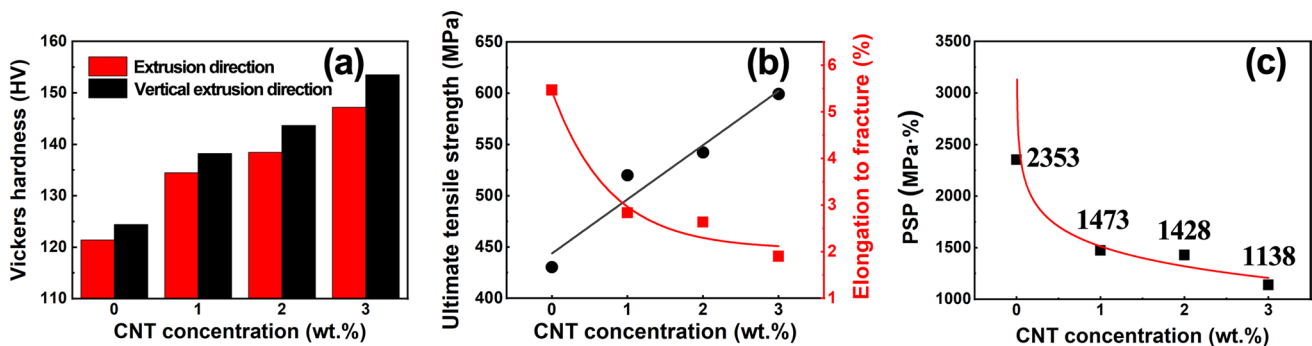

Fig. 5 **a** Vickers hardness, **b** tensile properties and **c** PSP of CNT/6061Al composites with different CNT concentrations

The product of strength and plasticity (PSP) of CNT/6061Al with different CNT concentrations are listed in Fig. 5c. It can be seen that the change of PSP was similar to that of El, namely the poor El of CNT/6061Al composites resulted in an inferior PSP. Especially, the PSP of 3 wt% CNT/6061Al composite was only half as that of 6061Al alloy.

3.2 Wear Properties of CNT/6061Al Composites

The friction coefficient and wear rate changing curves of CNT/6061Al composites with different CNT concentrations along different friction directions are presented in Fig. 6. It can be seen that the wear properties of CNT/6061Al composites showed clear dependence on the friction directions. The friction coefficient (Fig. 6a) and wear rate (Fig. 6b) show a similar changing trend with increasing CNT concentration along the CNT circumferential and CNT radial directions: namely, the friction coefficient and wear rate decreased firstly and then increased, and the minimum value was achieved at the CNT concentration of 2 wt%. However, the friction coefficient and wear rate showed a totally different changing trend along the CNT axial direction: the friction coefficient gradually decreased, while the wear rate increased with the increase of CNT concentration.

For the 6061Al alloy, the best wear resistance was obtained along the CNT axial direction (namely the extrusion direction), but the wear resistance got worse with the incorporation of CNT. That is, the CNT would worsen the wear resistance of 6061Al alloy along the CNT axial direction. However, for the CNT/6061Al, the best wear resistance was achieved along the CNT circumferential dirction, while the worst wear resistance was obtained along the CNT axial direction.

Figure 7 reveals the wear surface morphology of CNT/6061Al composites with various CNT concentrations along different friction directions. For the 6061Al alloy, the peeling pits had relatively small size and depth along the CNT axial direction (Fig. 7a, d and g), which was in accordance with the lowest wear loss. Delamination wear was the dominated wear mechanism for the matrix alloy during the wear process of reciprocating sliding.

For the CNT/6061Al composites, the wear surface was relatively smoother along the CNT circumferential and radial directions, as compared with that of the 6061Al alloy (Fig. 7b, c, e and f). With increasing CNT concentration, the size and depth of peeling pits decreased firstly and then increased, and the flattest wear surface was achieved at a CNT concentration of 2 wt%. The abrasive wear and delamination wear were the dominated wear mechanisms for the CNT/6061Al composites, when the friction direction was along the CNT circumferential and radial directions. As the friction test was along the CNT axial direction, the size and depth of peeling pits increased with increasing CNT concentration (Fig. 7h and i). And the dominated wear mechanism was delamination wear for the CNT/6061Al composite, when the friction direction was along the CNT axial direction.

For a better ways presenting the macro morphology of wear tracks, 3d profilograms along different friction directions are given in Fig. 8. It indicates that the maximum depth of wear tracks decreased firstly and then increased along the CNT circumferential and radial directions. As a result, the minimum depth was achieved at the CNT concentration of 2 wt%. But the depth of wear tracks increased with the increase of CNT concentration along the CNT axial direction. Further, the minimum depth for the 6061Al matrix alloy was achieved along the CNT axial direction,
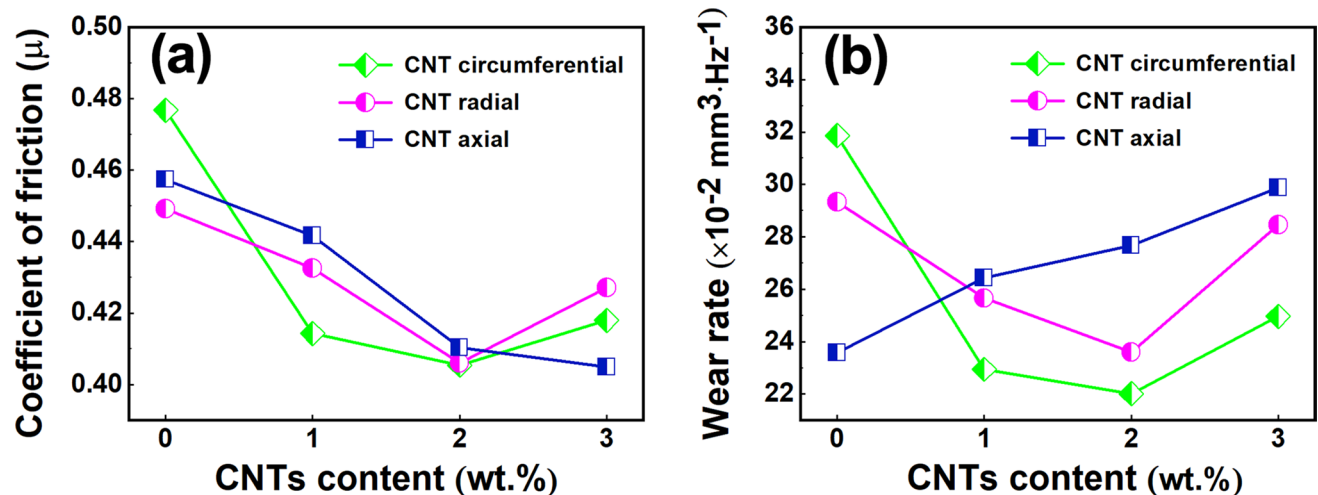

Fig. 6 Friction coefficient **a** and wear rate **b** changing curves of CNT/6061Al composites with different CNT concentrations along different friction directions
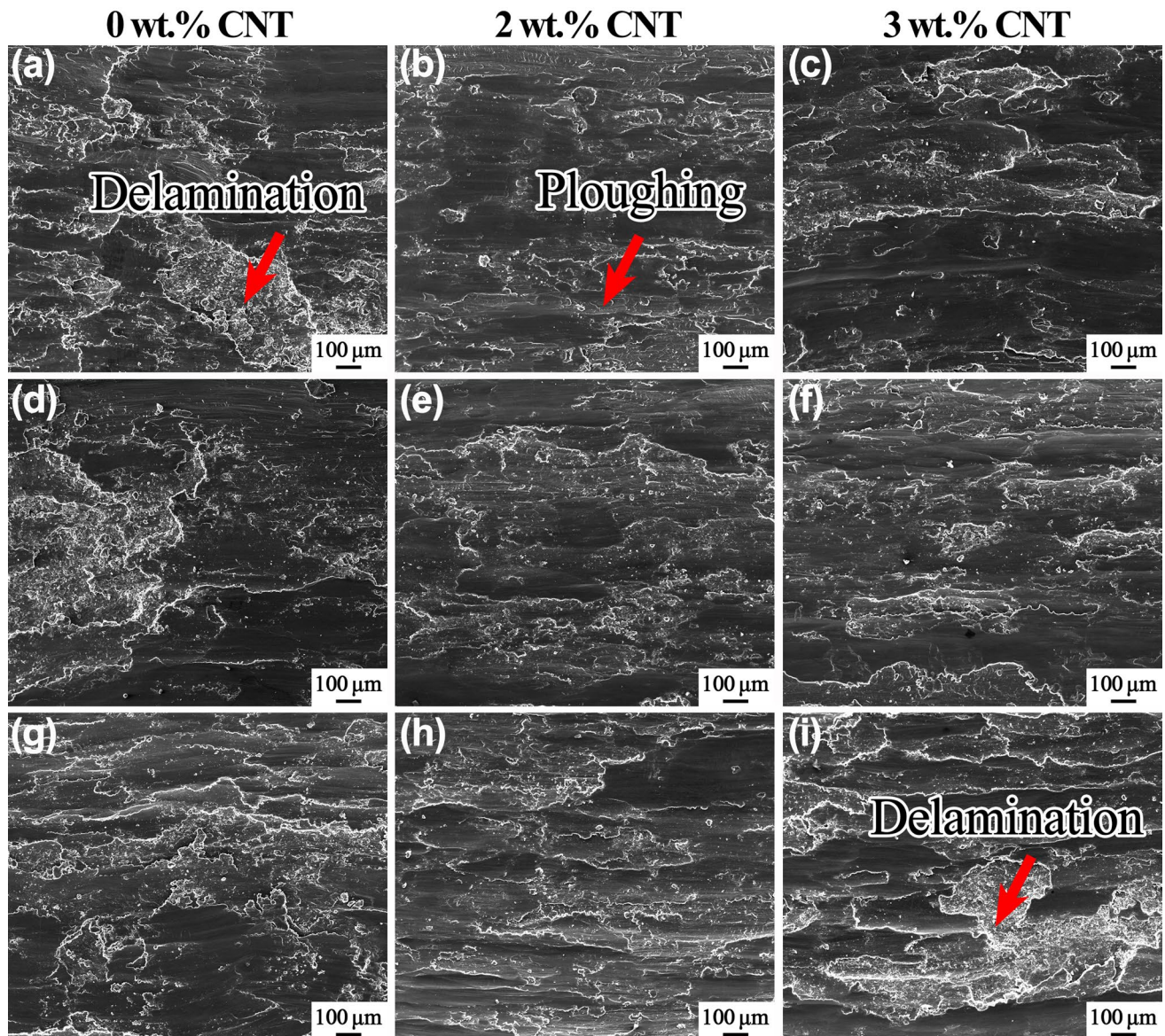
Fig. 7 SEM images of wear surfaces for CNT/6061Al composites with different CNT concentrations along different friction directions: **a–c** CNT circumferential direction, **d–f** CNT radial direction and **g–i** CNT axial direction

while the minimum depth for the CNT/6061Al composites was achieved along the CNT circumferential direction. These results were consistent with the wear rate change of CNT/6061Al composites, namely, the wear tracks usually exhibited a larger width and depth for the composites with poorer wear resistance.

4 Discussion

IT has been reported that the wear resistance of aligned CNT/epoxy composites was highly dependent on the wear directions [18]. Their study indicated that CNT/epoxy composites achieved the highest improvement of wear resistance along the CNT radial direction, whereas the least improvement was observed along the CNT axial direction. However, the wear anisotropy of CNT/6061Al composites was quite different (Fig. 6b). For the CNT/6061Al composite, the composite achieved the best wear resistance along the CNT circumferential direction. Especially, its wear resistance was even worse than the 6061Al alloy along the CNT axis direction. For analyzing the wear anisotropy of CNT/Al composites, the following analyses were carried out.
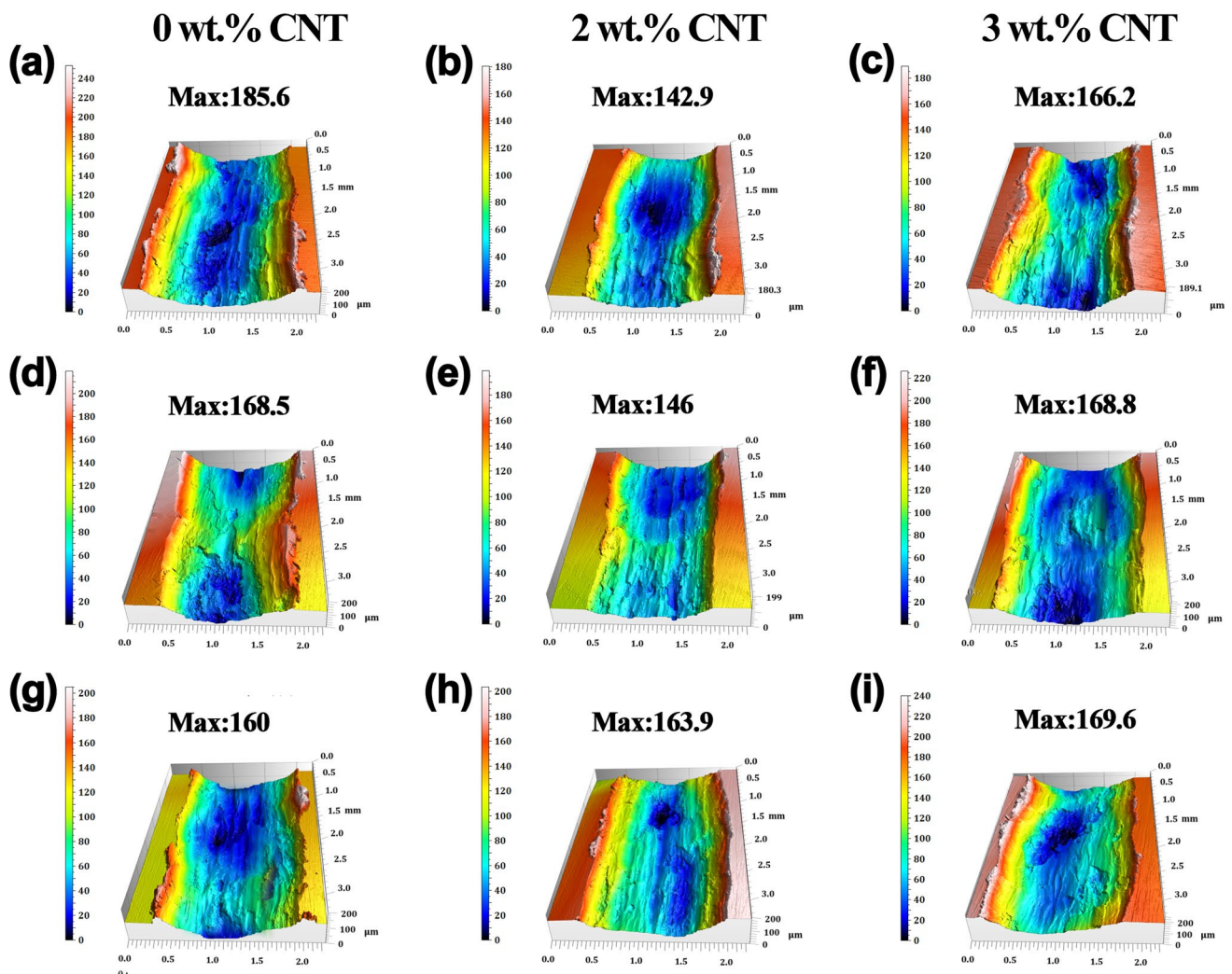
Fig. 8 3D morphologies of wear tracks for the CNT/6061Al composites with different CNT concentrations along different friction directions: **a–c** CNT circumferential direction, **d–f** CNT radial direction and **g–i** CNT axial direction. The maximum depth of wear tracks are also marked in this figure

4.1 Effect of CNT on the Wear Behavior of CNT/6061Al Composites

As reported by previous studies, the load transfer could enhance the strength and hardness of CNT/Al composites with the incorporation of CNT [20, 22–24], which could improve the wear resistant of CNT/6061Al composites. For analyzing the influence of load transfer of CNTs on the friction, FEM calculation under shear loading along different directions was carried out and the Mises stresses of the CNT and the Al matrix are shown in Fig. 9.

Two phenomena could be observed. Firstly, the Mises stress of the Al matrix was much lower than that of CNT. This was in accordance with the load transfer from Al matrix to CNTs. Secondly, the stress of the CNTs and Al matrix had the highest and lowest values, respectively, as the friction

shear direction was along the CNT radial direction. As the friction shear direction was along the CNT circumferential direction, the stress of the CNTs and Al matrix had the lowest and highest values, respectively. This indicates that the load transfer could be more effective, as the wear was along the CNT radial direction, thereby improving the wear resistance of CNT/6061Al composites. By comparison, the load transfer along CNT circumferential direction had a relative poor effect, which was not beneficial to increase the wear resistance. However, the CNT/6061Al composites actually exhibited the best wear resistance along CNT circumferential direction (Fig. 6b). This conflict indicates that the load transfer was not the main reason for the anisotropy for the wear behavior of CNT/6061Al composites.

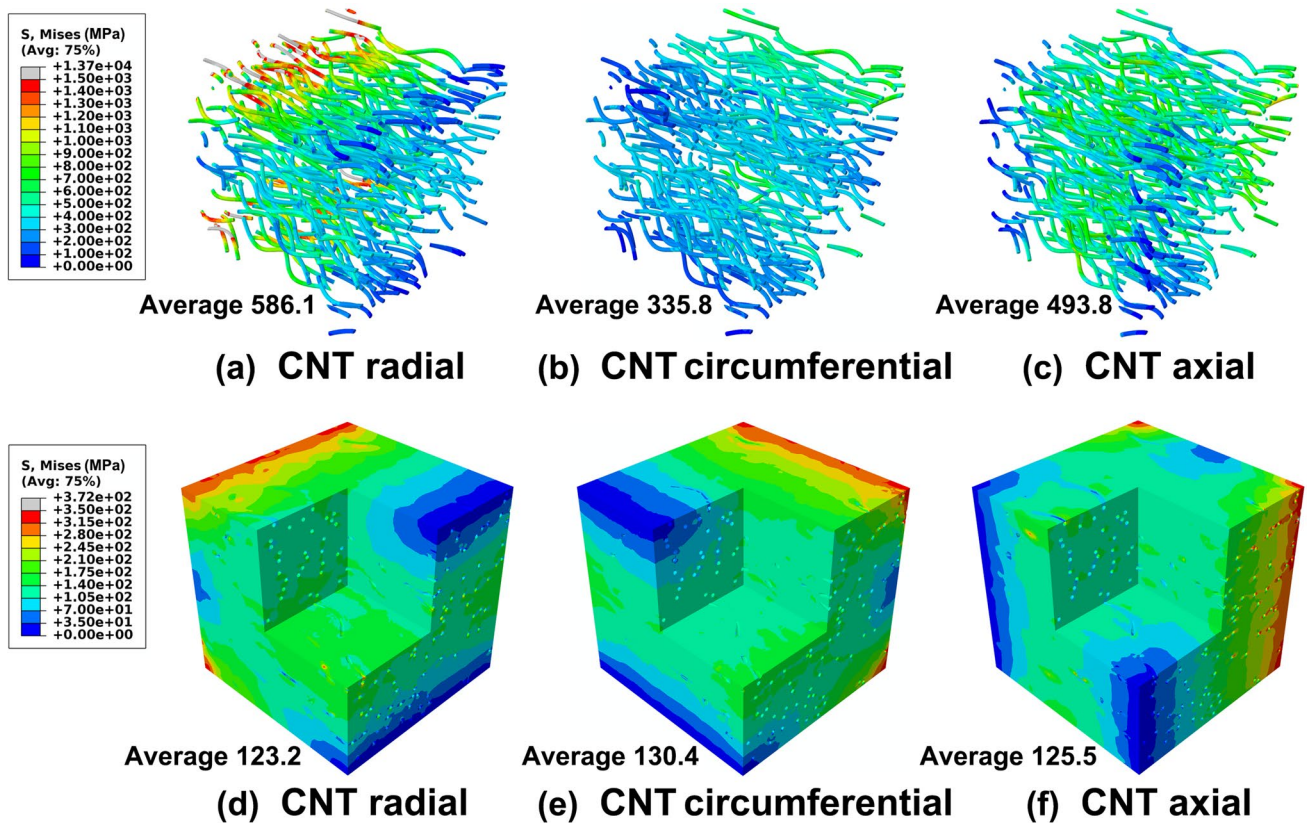The self-lubrication effect of CNT could also reduce the friction coefficient and wear rate of CNT/Al [9],

Fig. 9 The Mises stresses of **a**–**c** CNT and **d**–**f** 6061Al matrix along three different shear directions for 2 wt% CNT/6061Al composite

CNT/polymer [18, 25] and CNT/Ni composites [18, 26]. In general, the carbon would enrich the wear surface forming a 'carbon film' during the wear process, which could act as a solid lubricant enhancing the wear behavior significantly. In order to study the carbon content change of CNT/6061Al composites before and after the wear test along different friction directions, Raman spectral analysis was conducted on the wear surface (Fig. 10). It can be seen that the carbon content on the wear surface apparently increased, as the wear test was
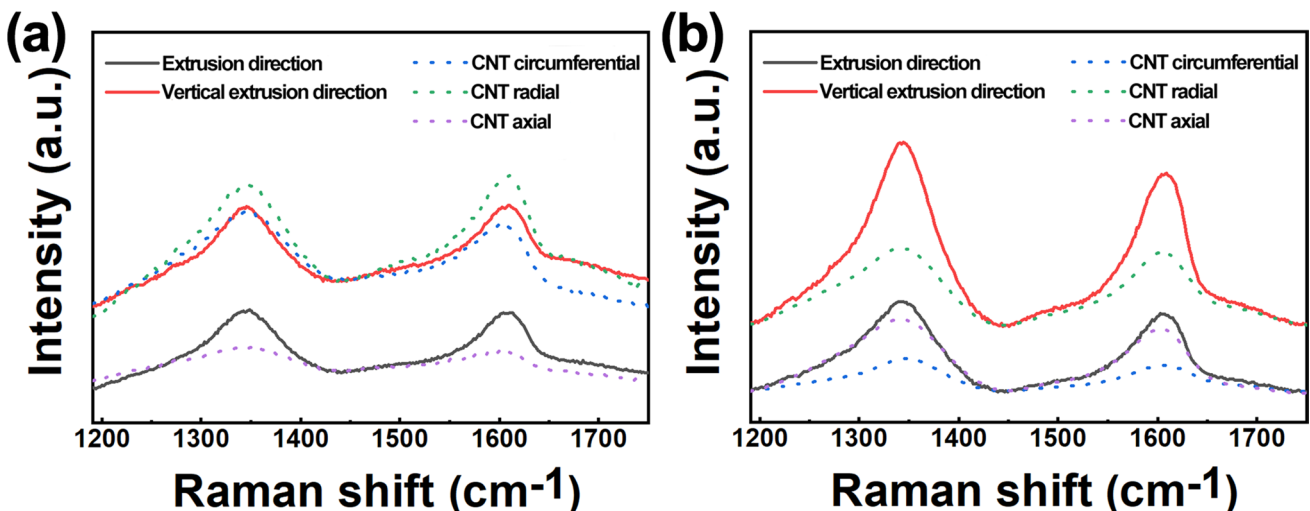

Fig. 10 Raman spectra of the **a** 2 wt% and **b** 3 wt% CNT/6061Al composites before and after the wear tests along different friction directions

along CNT circumferential or radial directions for the 2 wt% CNT/6061Al composite, while the carbon content reduced as the wear test was along the CNT axial direction. This indicates that the self-lubrication effect could well take effect along the CNT circumferential and radial directions, rather than the CNT axial direction.

For the 3 wt% CNT/6061Al composite, the carbon content decreased on the wear surface along different friction directions (Fig. 10b), indicating that the self-lubrication effect of CNT/6061Al composite was weakened when the CNT beyond a certain concentration. Previous research contributed this phenomenon to the presence of voids and cracks, which acted as a source for severe delamination wear [9, 13, 27]. Obviously, the presence of voids and cracks was not just the primary reason for the poor wear resistance in this study. The weakening of self-lubrication effect of CNT was believed to play a negative role for the wear resistance of the 3 wt% CNT/6061Al composite.

4.2 Effect of Grain Size on Wear Behavior

Figure 11 shows the grain size of the CNT/6061Al composites. It indicates that the grain size of CNT/6061Al composites slightly decreased with the incorporation of CNT along different directions. Further, the grain size decreased with increasing CNT concentration, and the minimum grain size was achieved at a CNT concentration of 3 wt%. This was mainly attributed to the effective pinning effect of the nano-sized CNT on the grain boundaries [28, 29].

On one hand, the refined grain would significantly increase the strength and hardness (Fig. 5a), which should be beneficial to improve the wear resistance to a certain extent. On the other hand, grain size had a significant effect on the toughness of nanocrystalline materials. It was reported the toughness of composites decreased with decreasing grain size, as the grain size was greater than 5 nm [30, 31]. The toughness of a material is defined as the PSP, which could effectively represent the ability to absorb energy in the plastic deformation before failure [32, 33]. Obviously, the
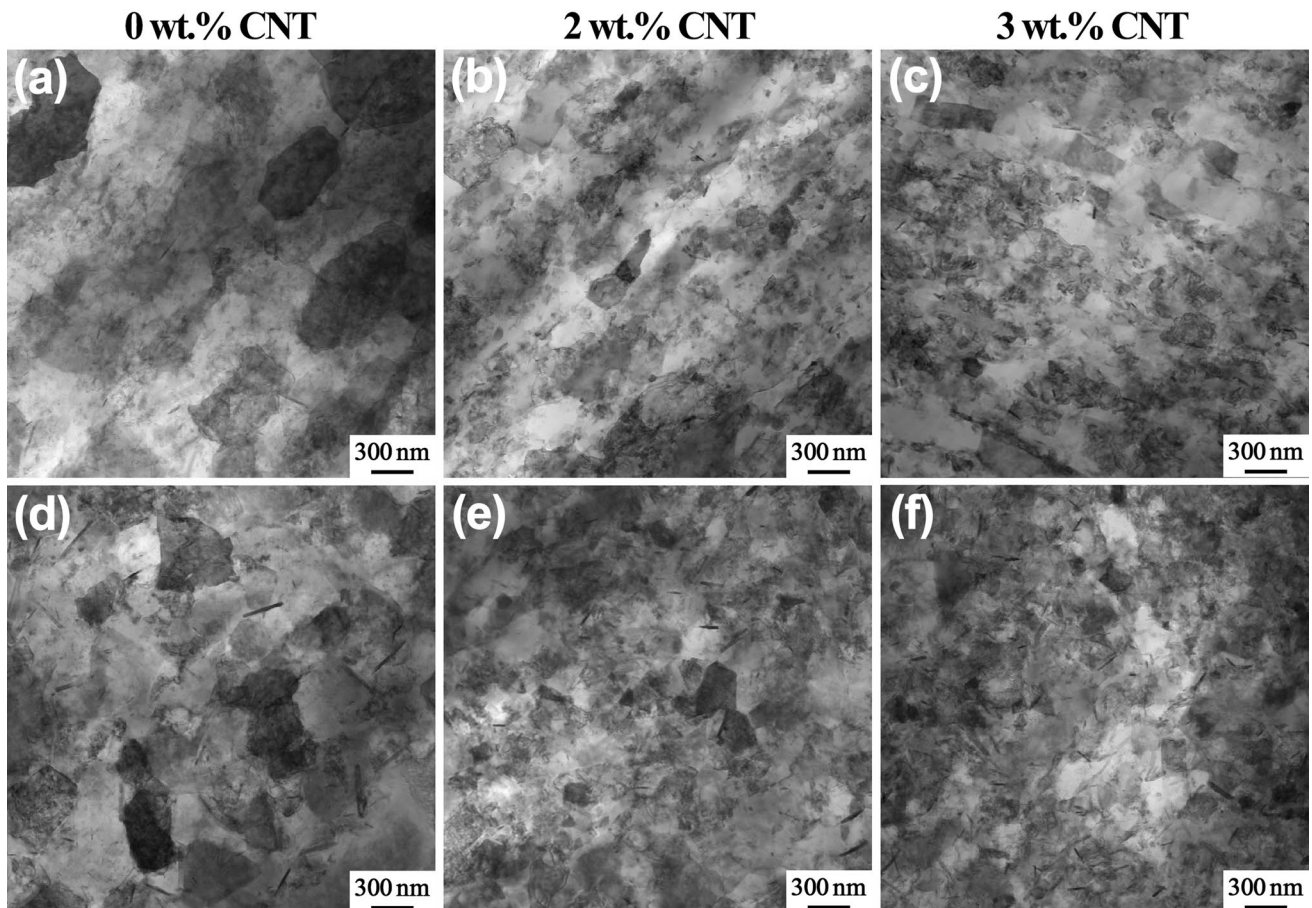

Fig. 11 Transmission electron microscopy (TEM) images showing grain structure of the CNT/6061Al composites with different CNT concentrations along: **a**–**c** extrusion direction and **d**–**f** vertical extrusion direction

deteriorated toughness of 3 wt% CNT/6061Al composite (Fig. 5c) would bring negative impact on the wear resistance [34, 35].

Two simple models for material removal during wear proposed by Moore et al. [35], give the material removal volume per unit contact area by plastic deformation mechanism:

$$V \approx 0.1\sigma/H \tag{1}$$

and by fracture mechanism:

$$V \approx 2\sigma^{5/4}d^{1/2}K_c^{-3/4}H^{-1/2} \tag{2}$$

where σ is the applied load per unit area (MN m^{-2}), H is the hardness (GN m^{-2}), d is the abrasive grit diameter (mm) and K_c is the fracture toughness (MN m$^{-3/2}$).

According to Eqs. (1–2), the fracture mechanism would cause about ten times as much wear volume as the plastic deformation mechanism. During the fracture process in brittle materials, the wear generally dominates in terms of 'block' slip, where shear takes place homogeneously and catastrophically across surfaces of maximum shear stress [34]. As a result, the severe delamination wear occurred (Fig. 7a, d and i). The grains of CNT/6061Al composites (Fig. 11) were gradually refined with the increase of CNT

concentration, which resulted in an inferior PSP and toughness (Fig. 5c). Materials in CNT/6061Al composites, especially the composite with high CNT concentration (3 wt%), were easily peeled off from the samples, and that was the main reason why the friction coefficient decreased while the wear rate gradually increased.

4.3 Effect of Texture on the Wear Behavior

After hot extrusion, the grain orientation was quite different along different directions. In order to study the grain orientation of CNT/6061Al composites, XRD pole figures were performed along extrusion and vertical extrusion directions. Figure 12 shows the pole figures and the orientation distribution function (ODF) section plot of the CNT/6061Al composites with different CNT concentrations along the extrusion direction. It can be seen that the CNT/6061Al composites had a typical fiber texture along the extrusion direction, and the maximum density value of texture significantly increased with increasing CNT concentration. This fiber texture was common for uniaxially deformed FCC metals with high stacking-fault energy [36]. Because CNT hinders grain boundary sliding [37], it needs more intracrystalline deformation to coordinate the deformation during
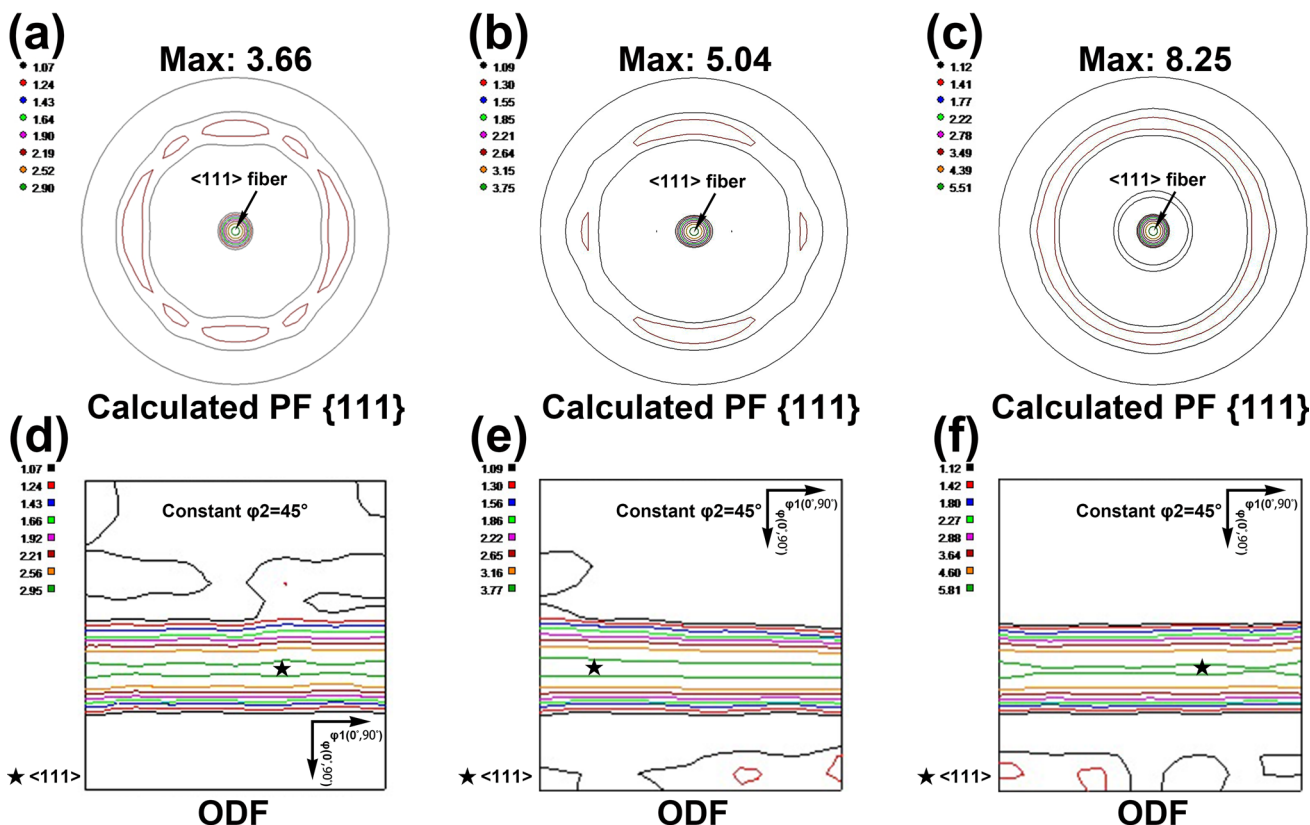

Fig. 12 Pole figures and ODFs of CNT/6061Al composites with different CNT concentrations along the extrusion direction: **a, d** 0 wt%, **b, e** 2 wt%, **c, f** 3 wt%

extrusion, which increases the density of the fiber texture. The increasing maximum density value of <111> fiber texture could provide CNT/6061Al composites a higher hardness (Fig. 5b) but lower plastic deformation capability with increasing CNT concentration [38].

The pole figures and ODFs of CNT/6061Al composites along the vertical extrusion direction are shown in Fig. 13. It can be seen that the dominant texture components were Brass {011} < 211 > and {112} < 110 > in the CNT/6061Al composites, for the three different composites. The maximum intensity of the main textures for CNT/6061Al composites along the extruded rod radial direction (namely the CNT radial direction) was significantly enhanced with the incorporation of CNT (Fig. 14). Further, the 3 wt% CNT/6061Al composite exhibited a lower maximum intensity of Brass {011} < 211 > and {112} < 110 > textures at $\varphi_2 = 45°$ than the 2 wt% CNT/6061Al composite. The

decrease in brass {011} < 211 > would weaken the plastic deformation capacity of material [39], and led to poor fracture strain. This was another reason for the poor wear resistance of 3 wt% CNT/6061Al composite along CNT circumferential and CNT radial directions.

Further, the CNT/6061Al composites along the vertical extrusion direction had the texture components of Brass {011} < 211 > and {112} < 110 > with higher Schmid factors of 0.41, while the composites along the extrusion direction had the texture component of < 111 > with lower Schmid factors of 0.27 (Fig. 14). It indicates that the sliding systems were easy to start along the vertical extrusion direction for the CNT/6061Al composites. Moreover, along the vertical extrusion direction, the texture intensity increased as increasing CNT concentration, indicating that the number of the grains with these favorable orientations was also increased. This would make it easier to start the
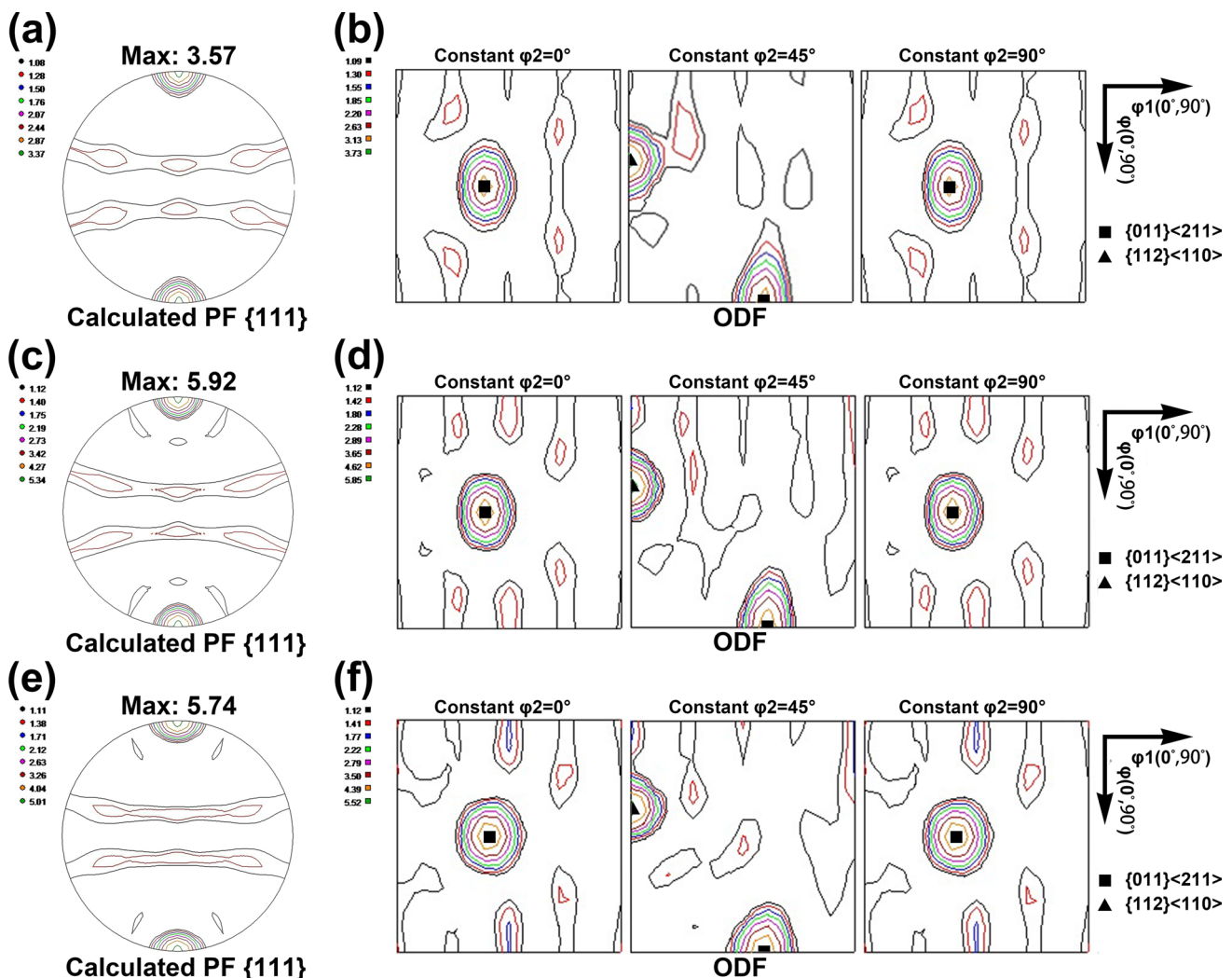

Fig. 13 Pole figures and ODFs of CNT/6061Al composites with different CNT concentrations along the vertical extrusion direction: **a, d** 0 wt%, **b, e** 2 wt%, **c, f** 3 wt%
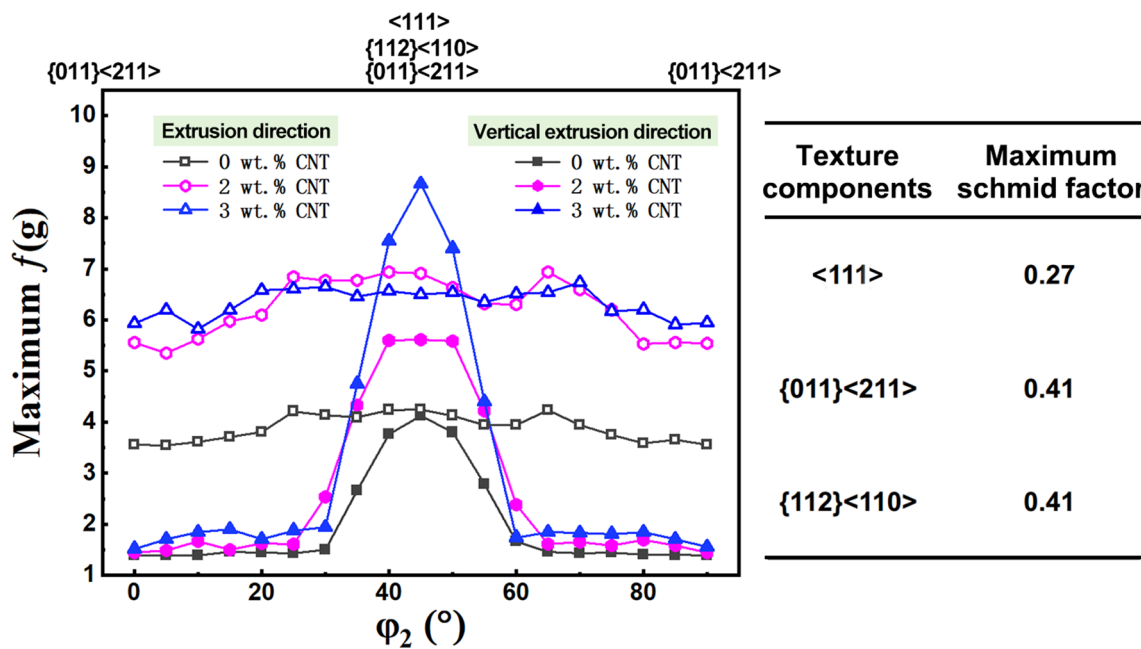
Fig. 14 Maximum intensity of main textures in CNT/6061Al composites with different CNT concentrations along the extrusion direction and vertical extrusion direction. The maximum schmid factors of the main texture components are also given

slip system under low stress. It means that the load transfer effect of CNT would be inhibited along the CNT radial direction during the wear process, resulting in worse wear resistance along the CNT radial direction.

From the above analysis, it can be seen that the grain refinement simply affected the wear behavior of CNT/6061Al composite with high CNT concentration (3 wt%), the influence on wear anisotropy of CNT/6061Al composites could be disregarded. The load transfer along the CNT radial direction was more effective than CNT circumferential direction (Fig. 9), but the CNT/6061Al composites actually exhibited the best wear resistance along CNT circumferential direction. This conflict indicates that the load transfer effect of CNT was not the main reason for the wear anisotropy of CNT/6061Al composites. Actually, the self-lubrication effect had a significant influence on the wear anisotropy, and the CNT could well take the self-lubrication effect along the CNT circumferential and radial directions, rather than the CNT axial direction. Further, with the incorporation of CNT, the maximum intensity of Brass {011} < 211 > and {112} < 110 > texture with high schmid factor significantly increased along the vertical extrusion direction, which made it easier to start the slip system under low stress. This means that the load transfer effect of CNT would be inhibited along the CNT radial direction during the wear process, resulting in worse wear resistance along the CNT radial direction, rather than the CNT circumferential direction.

5 Conclusions

In this work, the well-dispersed CNT/6061Al composites with directionally aligned CNTs were prepared through HEM combined with powder metallurgy technology, followed by hot extrusion. The effects of CNT and matrix structure on the wear behavior of the CNT/6061Al were investigated. The main conclusions can be drawn as follows:

1. The wear behavior of CNT/6061Al composites exhibited a significant anisotropy. The best and worst wear resistance was, respectively, obtained along the CNT circumferential and the CNT axial direction for the CNT/6061Al composites, which was quite different from those of the 6061Al alloy.
2. A certain CNT concentrations (1 wt% and 2 wt%) could effectively improve the wear resistance of CNT/6061Al composites, as the friction directions were along the CNT circumferential and CNT radial directions, as the result of the load transfer, grain refinement and self-lubrication effect of CNT. Along the vertical extrusion direction, the Brass {011} < 211 > and {112} < 110 > textures would inhibit the load transfer effect of CNT, resulting in a better wear resistance along CNT circumferential direction than the CNT radial direction.

3. Along the CNT axial direction, the weak deformability of composites caused by the synergistic effect of intensifying < 111 > fiber texture and refined grain size were the main reasons for the poor wear resistance of CNT/6061Al composites with increasing CNT concentration.

4. For the 3 wt% CNT/6061Al composites, because of the low toughness resulted from high CNT concentration, the deformability of the composite deteriorated significantly under the shear stress during the wear process. As a result, the wear resistance got worse, no matter what friction direction was.

Declaration

Conflict of interest The authors state that there are no conflicts of interest to disclose.

References

[1] K. Ma, Z.Y. Liu, K. Liu, X.G. Chen, B.L. Xiao, Z.Y. Ma, Carbon **178**, 190 (2021)

[2] Z.Y. Liu, B.L. Xiao, W.G. Wang, Z.Y. Ma, Carbon **50**, 1843 (2012)

[3] S.R. Bakshi, D. Lahiri, A. Agarwal, Int. Mater. Rev. **55**, 41 (2013)

[4] A. Krishnan, E. Dujardin, T.W. Ebbesen, P.N. Yianilos, M.M.J. Treacy, Phys. Rev. B **58**, 14013 (1998)

[5] M.F. Yu, B.S. Files, S. Arepalli, R.S. Ruoff, Phys. Rev. Lett. **84**, 5552 (2000)

[6] M.M.J. Treacy, T.W. Ebbesen, J.M. Gibson, Nature **381**, 678 (1996)

[7] S.Z. Zhu, D. Wang, B.L. Xiao, Z.Y. Ma, Compos. Pt. B-Eng. **212**, 108730 (2021)

[8] S.Z. Zhu, D. Wang, B.L. Xiao, Z.Y. Ma, Compos. Pt. B-Eng. **236**, 109851 (2022)

[9] H.J. Choi, S.M. Lee, D.H. Bae, Wear **270**, 12 (2010)

[10] R. Pérez-Bustamante, J.L. Bueno-Escobedo, J. Jiménez-Lobato, I. Estrada-Guel, M. Miki-Yoshida, L. Licea-Jiménez, R. Martínez-Sánchez, Wear **292**, 169 (2012). https://doi.org/10.1016/j.wear.2012.05.016

[11] A.M. Al-Qutub, A. Khalil, N. Saheb, A.S. Hakeem, Wear **297**, 752 (2013). https://doi.org/10.1016/j.wear.2012.10.006

[12] W.X. Chen, J.P. Tu, L.Y. Wang, H.Y. Gan, Z.D. Xu, X.B. Zhang, Carbon **41**, 215 (2003)

[13] I.Y. Kim, J.H. Lee, G.S. Lee, S.H. Baik, Y.J. Kim, Y.Z. Lee, Wear **267**, 593 (2009)

[14] S.M. Zhou, X.B. Zhang, Z.P. Ding, C.Y. Min, G.L. Xu, W.M. Zhu, Compos. Pt. A-Appl. Sci. Manuf. **38**, 301 (2007)

[15] X. Li, Z. Liu, Y. Zan, B. Xiao, D. Ni, Q. Wang, D. Wang, Z. Ma, Sci. China Technol. Sc **65**, 1149 (2022)

[16] X.N. Li, Z.Y. Liu, Z.X. Dai, H. Feng, B.Y. Xiao, D.R. Ni, Q.Z. Wang, D. Wang, Z.Y. Ma, Acta Metall. Sin. -Engl. Lett. **35**, 1765 (2022)

[17] Z.Y. Liu, B.L. Xiao, W.G. Wang, Z.Y. Ma, Acta Metall. Sin. -Engl. Lett. **27**, 901 (2014)

[18] H. Wang, L. Chang, X. Yang, L. Yuan, L. Ye, Y. Zhu, A.T. Harris, A.I. Minett, P. Trimby, K. Friedrich, Carbon **67**, 38 (2014)

[19] J.F. Zhang, X.X. Zhang, Z.Y. Liu, Q.Z. Wang, B.L. Xiao, Z.Y. Ma, Int. J. Mech. Mater. Des. **18**, 407 (2022)

[20] Z.Y. Liu, K. Ma, G.H. Fan, K. Zhao, J.F. Zhang, B.L. Xiao, Z.Y. Ma, Carbon **157**, 602 (2020)

[21] D. Singla, K. Amulya, Q. Murtaza, Mater. Today-Proc. **2**, 2886 (2015)

[22] H. Choi, G. Kwon, G. Lee, D. Bae, Scr. Mater. **59**, 360 (2008)

[23] F. Mokdad, D.L. Chen, Z.Y. Liu, B.L. Xiao, D.R. Ni, Z.Y. Ma, Carbon **104**, 64 (2016)

[24] S.R. Bakshi, A. Agarwal, Carbon **49**, 533 (2011)

[25] W.X. Chen, F. Li, G. Han, J.B. Xia, L.Y. Wang, J.P. Tu, Z.D. Xu, Tribol. Lett. **15**, 275 (2003)

[26] Z.H. Li, X.Q. Wang, M. Wang, F.F. Wang, H.L. Ge, Tribol. Int. **39**, 953 (2006)

[27] J.L. Jiang, H.Z. Wang, H. Yang, J.C. Xu, Trans. Nonferrous Met. Soc. China **17**, 113 (2007)

[28] S.C. Tjong, Mater. Sci. Eng. R-Rep. **74**, 281 (2013)

[29] C. Yuan, Z.Q. Tan, G.L. Fan, M.L. Chen, Q. Zheng, Z.Q. Li, J. Mater. Res. **34**, 2609 (2019)

[30] H. Feng, Q.H. Fang, L.C. Zhang, Y.W. Liu, Int. J. Plast. **42**, 50 (2013)

[31] Y. Liu, J. Zhou, T.D. Shen, D. Hui, Mater. Sci. Eng. A **528**, 7684 (2011)

[32] F. Huang, H. Zhang, J. Qi, Q. Chen, H. Ding, Mater. Res. Express **8**, 056510 (2021)

[33] F. Huang, Q. Chen, H. Ding, Y. Wang, X. Mou, J. Chen, Materials (Basel) **14**, 1121 (2021)

[34] B.R. Lawn, B.J. Hockey, H. Richter, J. Microsc. **130**, 295 (1983)

[35] H. Ding, X.P. Cui, Z.Q. Wang, J. Mater. Sci. Technol. **107**, 70 (2022)

[36] A. Bois-Brochu, C. Blais, F.A.T. Goma, D. Larouche, J. Boselli, M. Brochu, Mater. Sci. Eng. A **597**, 62 (2014)

[37] S. Bi, Z.Y. Liu, B.L. Xiao, Y.N. Zan, D. Wang, Q.Z. Wang, Z.Y. Ma, Mater. Sci. Eng. A **806**, 140830 (2021)

[38] M. Bastwros, G.Y. Kim, C. Zhu, K. Zhang, S. Wang, X. Tang, X. Wang, Compos. Pt. B-Eng. **60**, 111 (2014)

[39] V.K. Barnwal, R. Raghavan, A. Tewari, K. Narasimhan, S.K. Mishra, Mater. Sci. Eng. A **679**, 56 (2017)